Phase-Dependent Structure Sensitivity of Pt/TiO_2 for CO Oxidation Reactions

Haneul Kim, Kwang Hyun Kim, Konstantin Khivantsev, Joonwoo Kim, Jaekyoung Lee, and Ja Hun Kwak*

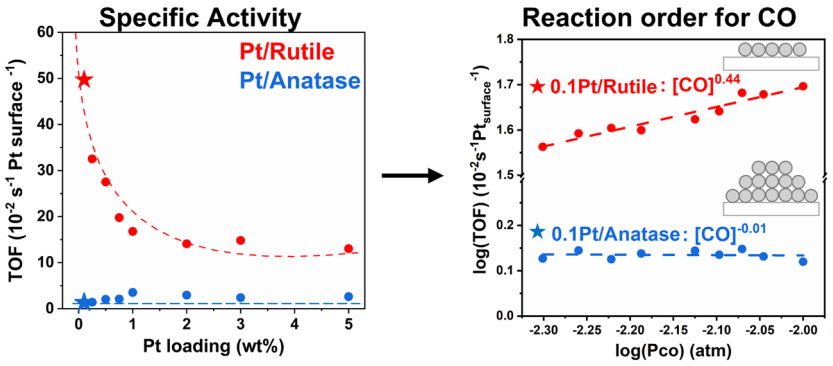

ABSTRACT: Here, we report the different structure sensitivity of Pt nanoparticles supported on titania (rutile vs anatase) for CO oxidation. The steady-state specific activity of Pt/rutile gradually increases with increasing Pt dispersion, while that of Pt/anatase remains unchanged regardless of Pt dispersion and is lower than that of Pt/rutile. Our kinetic studies demonstrate that the reaction order for CO is positive for subnm Pt clusters stabilized on rutile and gradually changes to zero for large Pt clusters (>1 nm). While Pt/anatase catalysts do not show dependency for CO concentration, irrespective of the size of the Pt nanoparticles. Scanning transmission electron microscopy (STEM), X-ray photoelectron spectroscopy (XPS), and CO chemisorption results confirm that the sintering of subnm Pt clusters supported on anatase occurs during the CO oxidation reaction, which is correlated with the change in the CO reaction order from positive (initially) to zero during the reaction. In contrast, subnm Pt clusters supported on rutile do not show significant sintering during the reaction but exhibit positive reaction order even at the steady state. Our study reveals the origin of the dramatic catalytic differences between Pt nanoparticles supported on anatase and rutile, highlighting the superior stability and activity of the Pt/rutile catalysts.

INTRODUCTION

The incomplete combustion of fossil fuels, such as exhaust from automobiles, thermal power plants, and steel mills, produces a significant amount of exhaust gas containing carbon monoxide (CO). Therefore, it is crucial to remove the emitted CO from the atmosphere for environmental and human health.[1−6] Pt and Pd/γ-Al_2O_3 catalysts are commonly used for CO removal through oxidation reactions due to their high activity and durability.[7−13] However, these catalysts have limitations, including rapid deactivation caused by sulfur poisoning and poor low-temperature activity. In this respect, Pt/TiO_2 catalysts have attracted considerable attention due to their superior low-temperature CO oxidation activity and high sulfur tolerance.[14−18] The CO oxidation reaction is also frequently employed as a model reaction to study supported metal catalysts and to understand the relationship between structure and catalytic properties.

Numerous studies have been conducted to investigate the low-temperature CO oxidation activity on Pt/TiO_2. It is well-known that Pt-based catalysts exhibit poor low-temperature activity due to CO poisoning, which arises from the strong interaction between CO and Pt.[19−21] However, Pt/TiO_2 can remain active at low temperatures due to unique active sites believed to involve the interfacial Pt sites on the TiO_2 support. Li et al. reported that the interfacial Pt sites are associated with the active sites for the reaction between CO and the surface oxygen of TiO_2.[22] DeRita et al. reported that single Pt atoms are active in low-temperature CO oxidation.[23,24]

The fraction of interfacial Pt sites is significantly influenced by the size of the Pt nanoparticles. In general, smaller Pt

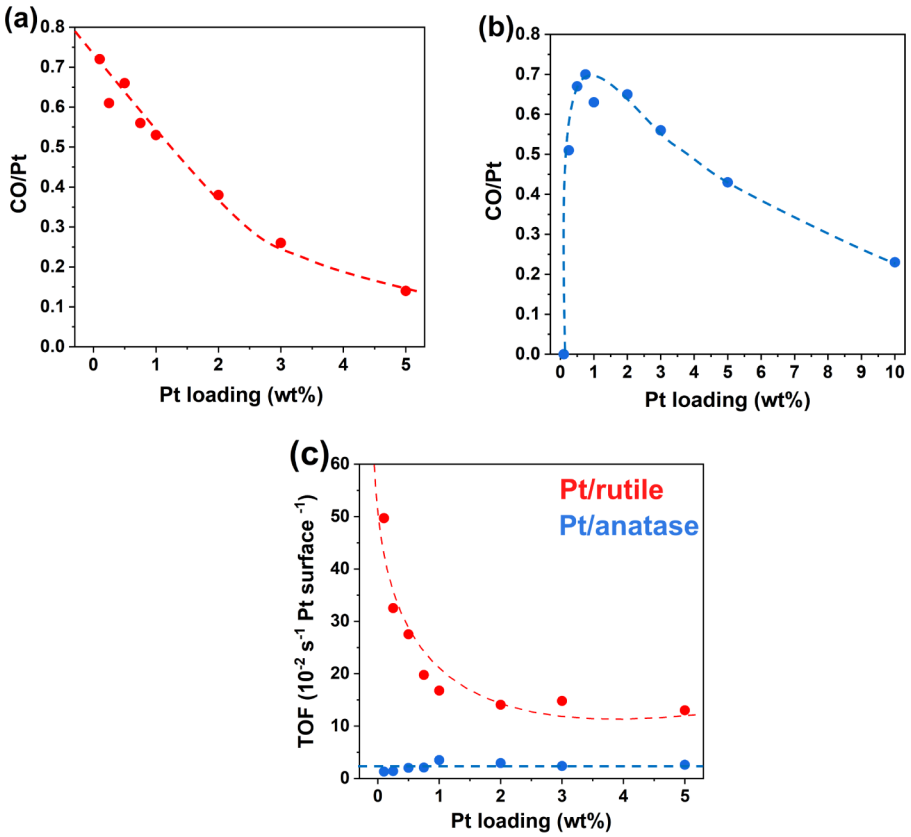

Figure 1. Pt dispersion for (a) Pt/rutile and (b) Pt/anatase using CO chemisorption at 40 °C, and (c) steady-state TOF for CO oxidation based on Pt dispersion.

clusters (including single Pt atoms) maximize the number of interfacial Pt sites, and they can be active during CO oxidation. Recently, Dessal et al. reported that the clustering of single Pt atoms during CO oxidation contributes to the high activity of Pt/Al_2O_3 for CO oxidation.[25] The effects of Pt particle size on the activity of Pt/TiO_2 for CO oxidation were also reported, indicating that the activity increases with decreasing Pt particle size.[22,24] On the contrary, it was also reported that smaller Pt clusters have stronger interactions with CO, which inhibit CO oxidation activity.[26−31] We thought that there are still many questions regarding the correlation between Pt size and activity for CO oxidation on rutile and anatase that remain unclear.[32−39]

In this study, we investigated CO oxidation on Pt nanoparticles supported by rutile and anatase to understand the effects of the Pt cluster size and support. The steady-state specific activities of the Pt/rutile catalysts increased as the Pt dispersion increased. However, there were no significant activity changes in Pt/anatase with Pt dispersion. Kinetic analysis of subnanometer Pt clusters supported on rutile showed a positive order with respect to CO, whereas Pt/anatase exhibited a zero order with respect to CO. CO chemisorption, STEM, and XPS clearly demonstrated that subnanometer Pt clusters on anatase titania sintered into 1−2 nm Pt clusters during the reaction, and it correlated with the reaction order changes from positive to zero for CO. On Pt/rutile, the Pt particles did not change under the reaction conditions, and the reaction order with respect to CO remained constant. These findings explain the differences in the observed reactivities of Pt nanoparticles supported by anatase and rutile titania for CO oxidation.

EXPERIMENTAL SECTION

Catalyst Preparation. 0.1−5 wt % Pt catalysts were prepared by the incipient wetness impregnation (IWI) of anatase (purity: 99.5%, average pore size (APS): 15 nm; US Research Nanomaterials, Stock No. US3492) and rutile (purity > 99.9%, APS: 30 nm; US Research Nanomaterials, Stock No. US3520) with a $Pt(NH_3)_4(NO_3)_2$ precursor in water (Figures S1 and S2). The samples were then dried at 110 °C for 30 min. Three impregnation-drying cycles were conducted to ensure a homogeneous distribution of Pt precursors. The samples were calcined under 20% O_2/He (60 sccm) at 400 °C for 2 h.

Catalyst Characterization. Hydrogen temperature-programmed reduction (H_2-TPR) was performed by using a Belcat-B instrument (BEL Japan, Inc.) equipped with a CATCryo instrument (BEL Japan, Inc.) and a thermal conductivity detector (TCD). A 50 mg catalyst sample was oxidized under 20% O_2/He (60 sccm) at 400 °C and cooled to 40 °C. The sample was then purged with He (60 sccm) for 30 min and stabilized under 2% H_2/Ar for 1 h at the same temperature. The sample temperature increased at 10 °C/min until it reached 700 °C. A 5A zeolite trap was used to trap water during the H_2-TPR.

CO chemisorption was conducted using a Belcat-B instrument (BEL Japan Inc.) under 10% CO/He (60 sccm) at 40 °C. The catalysts were oxidized under 20% O_2/He (60 sccm) at 400 °C for 2 h, followed by reduction under 10% H_2/He (60 sccm) at 200 °C for 1 h. After being purged with He (60 sccm) at 300 °C, the catalysts were cooled to 40 °C. For the used catalyst, the catalysts were treated at 80 °C under a mixture of 1% CO and 2.5% O_2 in He gas conditions for 2 h. The samples were then reoxidized, rereduced, and cooled

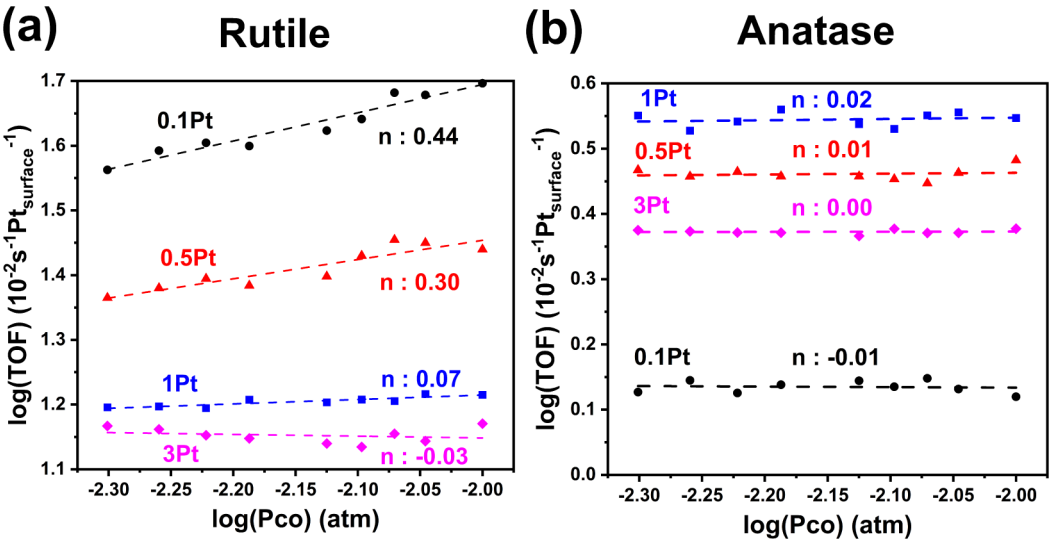

Figure 2. Steady-state activity of CO oxidation at 80 °C as a function of CO concentration on (a) Pt/rutile and (b) Pt/anatase.

under the same conditions as mentioned above. The amount of consumed CO during the chemisorption experiment was estimated as the total amount of adsorbed CO on Pt. To correct for overestimation due to physisorbed CO, secondary CO adsorption was conducted after He purging at the same temperature. The amount of consumed CO from this secondary experiment represented the amount of physisorbed CO, and it was subtracted from the initial CO uptake to obtain the amount of chemisorbed CO on Pt. A 1:1 CO/Pt stoichiometry was assumed to calculate the metal dispersion. Detailed information for estimating the particle size of Pt from the CO chemisorption results can be found in the Supporting Information.

High-angle annular dark-field scanning transmission electron microscopy (HAADF-STEM) images were acquired by using a JEOL JEM-2100F microscope operating at 200 kV.

The XPS spectra of fresh and used Pt/TiO_2 were obtained using K-alpha (PHI 5000 VersaProbe, Physical Electronics, Inc., Chanhassen, MN, USA) with Al Kα (1486.6 eV). The XPS profiles were corrected with reference to the C 1s peak at 284.6 eV.

Catalytic Reaction Test. All catalytic reaction tests were performed using 20 mg of the sample in 1% CO and 2.5% O_2 in He (60 sccm) gas. For the temperature-programmed reaction (TPRx), the reaction gas mixture was introduced for 10 min at RT and then ramped to 300 °C at a rate of 5 °C/min. The CO oxidation activity was monitored over a 2 h period at 80 °C to calculate the turnover frequency (TOF) and reaction order. The samples were diluted with bare SiO_2, and the effluent gases were analyzed by using gas chromatography (GC). The TOF was calculated based on the surface-exposed Pt, normalized by CO/Pt from CO chemisorption. For the CO reaction order of the Pt/TiO_2 catalyst, a CO oxidation reaction was conducted by feeding 0.5−1% CO in a 2.5% O_2/He balance gas, using TOF measurements for the initial and steady states. The TOF for the initial state was calculated by extrapolating the data from 3−13 min. The TOF for the steady state was calculated after 2 h of reaction. For the O_2 reaction order of the Pt/TiO_2 catalyst, a CO oxidation reaction was conducted by feeding 1%−10% O_2 in 1% CO/He balance gas, using TOF measurements for the steady state.

RESULTS AND DISCUSSION

To investigate the impact of Pt size on the CO oxidation reaction, we synthesized Pt supported on rutile and anatase with different Pt loadings (0.1−5 wt %) and denoted them as *X*Pt/support (*X* = wt % of Pt). All synthesized catalysts were calcined at 400 °C and reduced at 200 °C based on our previous report and H_2-TPR results (Figure S3).[36] We further performed CO chemisorption to determine the Pt dispersion of the samples.[40,41] Both Pt/rutile and Pt/anatase samples showed that the Pt dispersion increased as the Pt loading decreased (Figure 1a). However, at low Pt loading (≤0.5 wt %), Pt/anatase exhibited a significant decrease in CO/Pt as the Pt loading decreased. This trend was more evident for 0.1Pt/anatase, which showed no detectable CO adsorption (Figure 1b), suggesting the formation of single-atom (SA) Pt that does not adsorb CO at 40 °C.[23,24] The 0.25Pt/anatase sample contained both SA and small clusters, while only the Pt clusters contributed to the CO adsorption (Figure S4). The relative distributions were presented as CO/Pt ratios, and we estimated the Pt size using CO chemisorption and STEM images (detailed information in the Supporting Information).

We conducted TPRx experiments using Pt/TiO_2 catalysts to compare the CO oxidation activity of the catalysts (Figure S5and Table S1). Pt/rutile samples showed a similar T_{50} (temperature for 50% CO conversion) with a difference of approximately ∼20 °C as the Pt loading increased, while the T_{50} of Pt/anatase samples decreased with an increase in Pt loading. To quantitatively compare the effects of Pt dispersion on specific activity, a time-on-stream reaction was conducted at 80 °C, which is near the onset temperature of CO oxidation. During the reaction, the activity of the Pt/rutile catalyst increased slowly and reached a steady state within 2 h. The activity of Pt/anatase exhibited an initial deactivation period and then achieved a steady state. The specific activity was estimated from the turnover frequency (TOF) of Pt/TiO_2 determined based on a CO/Pt (Figures 1c andS6). We need to note that the Pt dispersion of 0.1Pt/anatase used the CO chemisorption results after 2 h of the CO oxidation reaction (CO/Pt = 0.51) due to the absence of CO adsorption on a fresh catalyst consisting mainly of single atoms. The TOF of Pt/rutile increased dramatically as the Pt particle size

decreased. However, the TOF of the Pt/anatase samples did not change significantly with Pt dispersion. The TOF results provide evidence of the structural sensitivity of Pt/rutile and the structural insensitivity of Pt/anatase. The structural sensitivity of Pt supported on various supports for CO oxidation has been discussed intensively. Boudart and Rumpf reported that Pt-based catalysts are structure insensitive for CO oxidation.[42] Cant et al. reported that Pt/SiO_2 is structure insensitive for CO oxidation.[43] Allian et al. also reported that Pt/γ-alumina shows structure insensitivity because CO binding strength determines the activity, independent of Pt size.[44] However, Cargnello et al. reported that Pt/CeO_2 is structure sensitive because of the crucial role of the Pt perimeter sites. They reported that the Pt perimeter sites on CeO_2 are the active sites and that CO adsorbed on Pt combines with oxygen at the metal-ceria interface.[45] Li et al. also reported that the specific activity of Pt/TiO_2 was proportional to the Pt dispersion because the interfacial Pt atoms were the active sites.[22] Based on the literature, Pt on nonreducible supports, such as SiO_2 or Al_2O_3, shows structural insensitivity; that is, the specific activity is independent of the Pt size. Meanwhile, Pt on reducible supports, such as CeO_2 and TiO_2, shows structural sensitivity to CO oxidation. Interestingly, our study reports for the first time that even on the same reducible TiO_2 supports, structure sensitivity can be different: structure sensitive on Pt/rutile and structure-insensitive on Pt/anatase.

Kinetic measurements were conducted on both Pt/rutile and Pt/anatase catalysts to identify the differences in structural sensitivity between these catalysts. The steady-state turnover frequencies were determined by varying the CO concentration from 0.5 to 1% while maintaining the O_2 concentration at 2.5% (Figure 2). For the Pt/rutile catalyst (Figure 2a), the reaction order for the 0.1Pt and 0.5Pt catalysts was 0.44 and 0.30, respectively. When the Pt dispersion decreased to 0.53 (1Pt/rutile), the reaction order for CO became zero. In contrast, for Pt/anatase (Figure 2b), the reaction order for CO was zero, regardless of Pt loading and dispersion. The reaction order for O_2 was positive for all Pt/TiO_2 samples, which is consistent with previous reports (Figure S7).[23,24]

Previous studies on Pt-based catalysts have reported a negative or zero reaction order for CO and a positive reaction order for O_2, which is assumed to be related to the CO poisoning effect.[42,44,46] Cargnello et al. and DeRita et al. reported that Pt on TiO_2 and CeO_2 shows a zero reaction order for CO, and its reactivity depends on Pt size.[23,45] Notably, our results show that subnanometer-sized Pt particles supported on rutile show a positive reaction order, whereas Pt/anatase shows a zero reaction order for CO, even though both 0.5Pt/anatase and 1Pt/anatase possess similar Pt dispersions of 0.56 and 0.63, and 0.1Pt/rutile and 0.5Pt/rutile have dispersions of 0.72 and 0.67, respectively. Therefore, this difference did not simply stem from the size of the Pt clusters.

CO chemisorption was performed on the Pt/TiO_2 samples after the reaction to understand the dispersion changes of Pt during the reaction (Table 1). For Pt/rutile, the Pt dispersion values are practically the same, ranging from 0.5 to 0.8 between freshly prepared and used catalysts. This result suggests that the Pt clusters remained stable on the rutile support and did not sinter appreciably. For Pt/anatase, the Pt dispersion changed notably from ~0 to 0.51 for 0.1Pt/anatase. Since there is no CO adsorption on fresh 0.1Pt/anatase because single Pt atoms are the dominant Pt sites, 0.1Pt/anatase shows apparent Pt sintering of single Pt atoms into Pt clusters whose

Table 1. Pt Dispersion of CO/Pt: Pt/rutile and Pt/anatase Calculated by CO Chemisorption Data

Sample	Status/Pt loading	Fresh	Used
Rutile	0.1 wt %	0.72	0.82
	0.5 wt %	0.56	0.69
	1 wt %	0.53	0.62
Anatase	0.1 wt %	-	0.51
	0.5 wt %	0.67	0.59
	1 wt %	0.63	0.59

average sizes are 1−2 nm. The Pt dispersion of the 0.5 and 1Pt/anatase samples did not change significantly. Even with similar Pt dispersion values in the 0.5Pt/rutile and 0.5−1Pt/anatase samples, the reaction order for CO was significantly different (0.3 versus 0). These results demonstrate that the difference in the reaction order for CO does not simply originate from the Pt size difference but that the titania support largely contributes to it.

Scanning transmission electron microscopy (STEM) measurements were conducted to confirm changes in the Pt size during the reaction. For the freshly prepared 0.1Pt/rutile catalyst, Pt predominantly existed as subnm clusters, while 0.1Pt/anatase mainly contained single Pt atoms (Figure 3a−d). After a 2 h reaction, the size of the Pt clusters in 0.1Pt/rutile did not change significantly compared with the freshly prepared sample. However, after the reaction test, 0.1Pt/anatase mostly contained ~1 nm Pt clusters, which is consistent with the CO chemisorption results (Figure 3e−h). The particle size distribution of 0.1Pt/rutile from STEM images shows subnanometer Pt clusters for both the freshly prepared sample and after the 2 h reaction, while after 2 h reaction, 0.1Pt/anatase clearly shows average ~1 nm Pt clusters, which are much larger than those on the 0.1Pt/rutile sample (Figure 3). For 0.5Pt/rutile, the analysis confirms the coexistence of subnanometer and 1−2 nm Pt clusters before and after the reaction (Figure S8). For 1Pt/anatase and 1Pt/rutile, the particle size distribution of fresh 1Pt/rutile and anatase from STEM showed ~1 nm Pt clusters that do not change even after 2 h reactions (Figure S9). STEM images allowed us to infer that the subnm Pt clusters on rutile titania show a positive reaction order in CO, while ~1 nm Pt clusters exhibit zero order. Pt/anatase samples show zero order in CO for ~1 nm Pt clusters.

The X-ray photoelectron spectroscopy (XPS) results also support the conclusion that sintering of Pt clusters on 0.1Pt/anatase occurred during the reaction (Table 2). For freshly prepared 0.1Pt/anatase, only the Pt oxidic phase was present, and its oxidation state was similar to the SA Pt structure, such as Ti−O−Pt(II)−O−Ti reported by Nagai et al. (Figure 4a,−b).[17] However, after the reaction, 0.1Pt/anatase showed the coexistence of metallic Pt and Pt oxidic phases, and STEM confirmed the existence of 1−2 nm Pt clusters. In conclusion, the reduction by CO during the reaction is one of the reasons for the Pt sintering. Both 0.1Pt/rutile samples before and after the reaction show a similar metallic Pt ratio (Figure 4c,d). The XPS data for other samples also provide evidence that metallic Pt and Pt oxidic phases coexisted before and after the reaction (Figure S10and Table S2). And we could not find any signal corresponding to the Al 2p, which is well-known to overlap with Pt^{4f}, indicating that there was no detectable Al contamination in the TiO_2 samples (Figure S11).

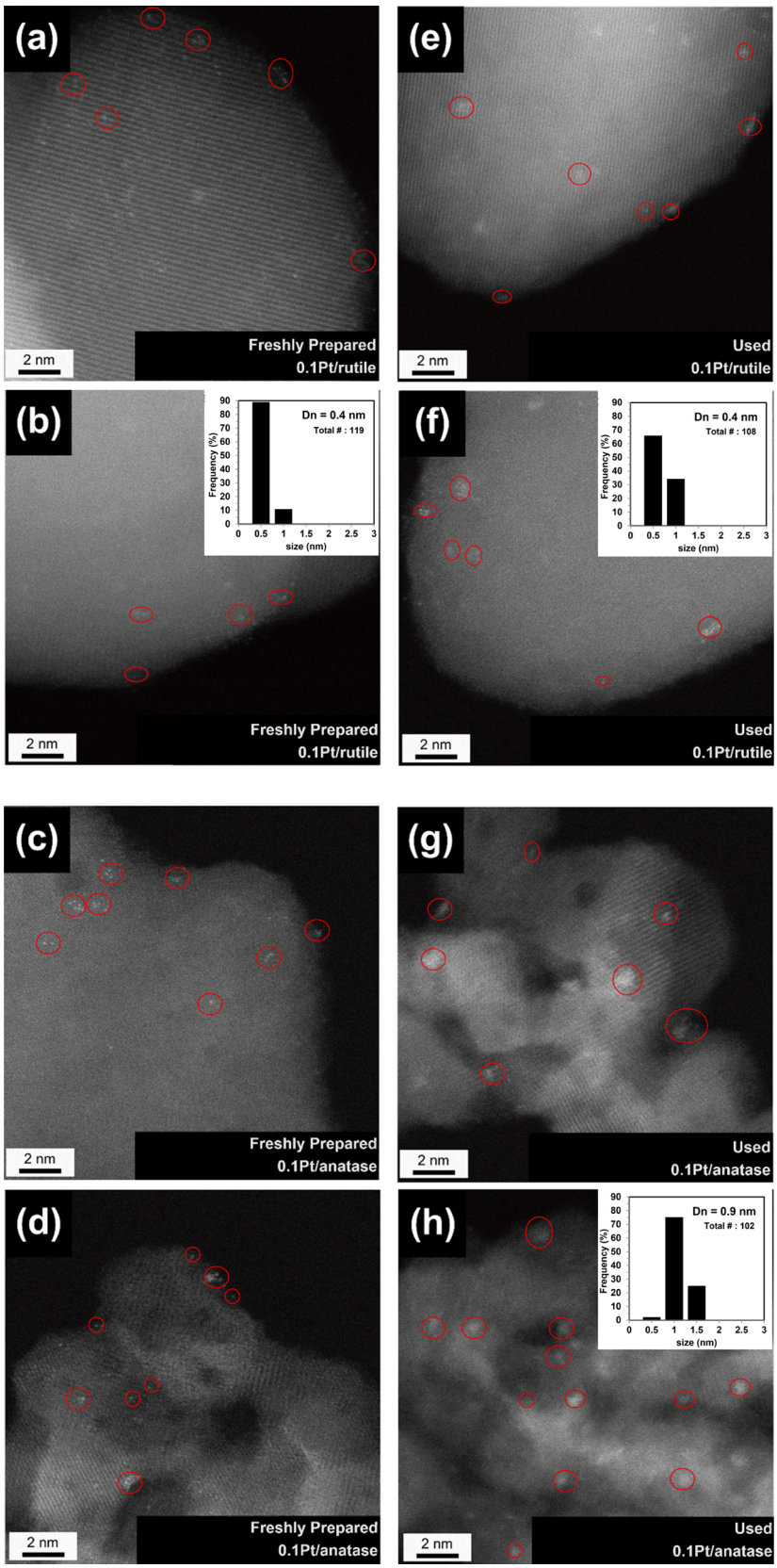

Figure 3. STEM images of freshly prepared (a, b) 0.1Pt/rutile and (c, d) 0.1Pt/anatase, and used (e, f) 0.1Pt/rutile and (g), (h) 0.1Pt/anatase.

We extrapolated the initial reaction rates and estimated the reaction order of freshly prepared small Pt clusters, excluding the effect of changes in the Pt cluster size during the reaction (Figures S12 and S13). Freshly prepared 0.1Pt/rutile and 0.1Pt/anatase exhibited positive reaction orders for CO: 0.49 and 0.33, respectively, consistent with the results of Celine et al.[47] Importantly, 0.1Pt/anatase showed a positive reaction order initially but changed to zeroth order at the steady state

Table 2. Metallic Pt (Pt^0) Ratio of 0.1 Pt/rutile and 0.1 Pt/anatase Calculated by XPS Spectra

Sample	Fresh	Used
0.1Pt/rutile	0.27	0.32
0.1Pt/anatase	0.00	0.082

(Figure 5). These results are attributed to changes in the Pt particle size during the CO oxidation reaction. In the low Pt loading region (up to 1 wt %) of the rutile-supported samples, the subnm Pt clusters remained stable during the reaction, and keep the positive reaction order for CO and a higher specific activity for CO oxidation. Pt/anatase, on the other hand, sintered into 1−2 nm Pt clusters during the reaction, which showed a zeroth reaction order for CO.

The question remains is why the subnanometer Pt clusters on TiO_2 (whose size is visualized by microscopy) do not show better dispersion than 1−2 nm sized Pt clusters,, similar measured CO/Pt chemisorption values. We thought this is related to the presence of an oxidic Pt phase, as evidenced by the XPS data, which makes it hard to decouple since it does not adsorb CO at 40 °C. Based on the STEM results, we inferred that the subnanometer Pt clusters exhibit a 2D raft-like structure, whereas the 1−2 nm Pt clusters exhibit a 3D structure. 2D raft-like Pt clusters have relatively weak interactions between Pt and CO compared to 3D Pt particles (Figure S14). We hypothesize that 2D raft-like Pt clusters have relatively weak interactions between Pt and CO compared to 3D Pt particles. As shown in detailed kinetic studies (Figure 6), the apparent activation energies for CO oxidation on 0.1Pt/rutile were 17 kJ/mol, while those on 0.1Pt/anatase were 55 kJ/mol. Compared to 1Pt/rutile and 1Pt/anatase, 0.1Pt/rutile shows twofold lower activation barrier than 1Pt/rutile (35 kJ/mol), whereas 0.1Pt/anatase shows a similar activation barrier to 1Pt/anatase (55 kJ/mol). The activation barrier value of 17 kJ/mol is significantly lower than the activation energies of typical Pt-based catalysts (40−60 kJ/mol).[23,29,36,44,47] This unusually low activation barrier of 0.1Pt/rutile might be related to the morphology of subnanometer Pt supported on rutile. We conduct ongoing research focused on understanding the unique CO oxidation activity of subnanometer Pt supported on rutile. This study includes a detailed investigation of the mechanism using density functional theory (DFT) calculations and infrared (IR) measurements.

CONCLUSIONS

We studied the effects of the Pt size and titania support on the CO oxidation reaction of titania-supported Pt catalysts. The steady-state specific activity of Pt/rutile increased gradually as the Pt dispersion increased, whereas the specific activity of Pt/anatase remained constant regardless of the Pt dispersion. Kinetic experiments demonstrated that subnanometer Pt clusters on rutile showed a positive reaction order in CO. On the other hand, 3D clusters measuring ∼1 nm on rutile exhibited a zeroth reaction order for CO, which is typical for Pt nanoparticles. Pt/anatase showed a zeroth reaction order in CO, irrespective of the Pt loading and dispersion. The CO chemisorption, STEM, and XPS results confirmed that subnanometer Pt clusters on rutile remained stable during the reaction, while for Pt/anatase, the Pt clusters sintered into ∼1 nm particles, exhibiting a typical zeroth reaction order in

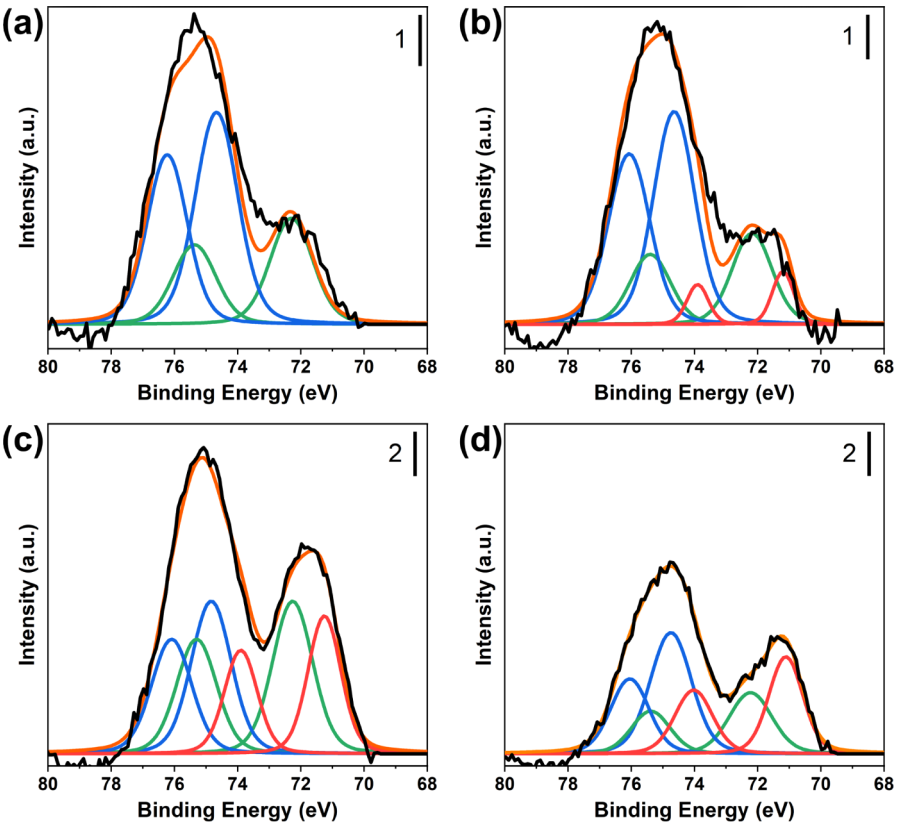

Figure 4. XPS spectra of (a) freshly prepared and (b) used 0.1Pt/anatase, and (c) freshly prepared and (d) used 0.1Pt/rutile. Black line: Original signal, Orange line: Fitted signal, Red line: Pt^0, Green line: Pt^{2+}, Blue: Pt^{4+}).

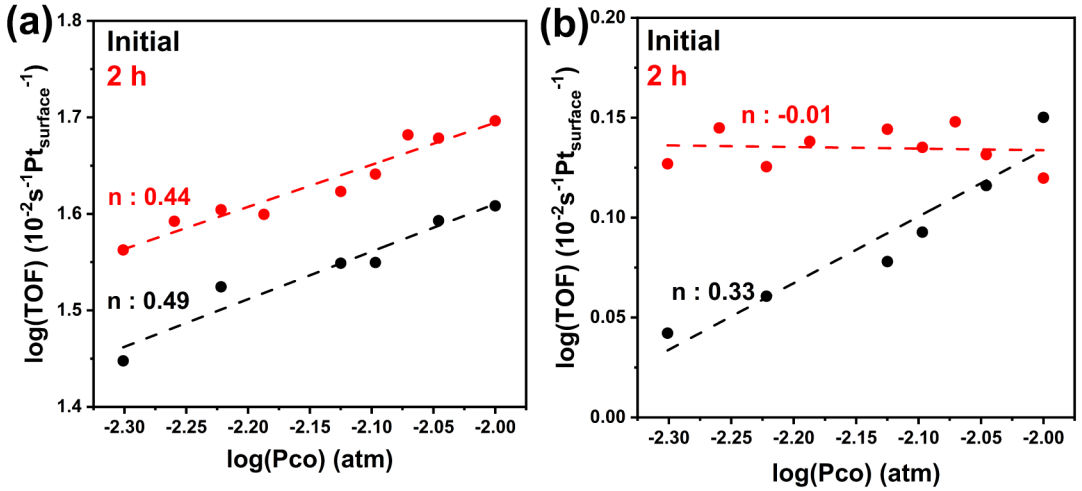

Figure 5. Initial and steady-state activity as a function of CO concentration on (a) 0.1Pt/rutile and (b) 0.1Pt/anatase.

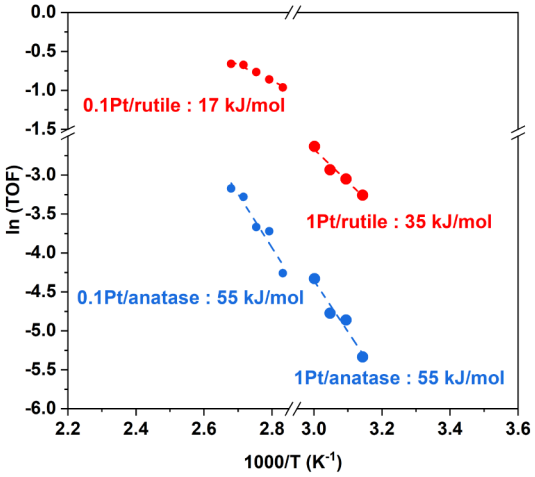

Figure 6. Arrhenius plots of 0.1Pt/rutile, 0.1Pt/anatase, 1Pt/rutile, and 1Pt/anatase.

CO. The initial reaction orders in CO for 0.1Pt/rutile and 0.1Pt/anatase were 0.49 and 0.33, respectively. However, the steady-state reaction orders changed to 0.44 and zero, respectively. This change occurred due to the sintering of Pt clusters on anatase titania during the reaction. These sintered Pt clusters had a 3D structure and a stronger interaction with CO compared to subnanometer Pt clusters, which had a 2D raft-like morphology. These morphological differences can be attributed to the disparities in the Pt interaction strength between the anatase and rutile titania surfaces. Overall, subnanometer Pt clusters showed a positive reaction order in CO with higher CO oxidation activity, whereas Pt clusters larger than 1 nm showed a zeroth reaction order with lower CO oxidation activity.

■ ASSOCIATED CONTENT

Supporting Information

T_{50} in CO oxidation, Pt^0 ratio calculated by XPS spectra, and interpretation of XPS spectra of Pt/rutile and Pt/anatase. Detailed information for Pt size calculations, XRD patterns and H_2-TPR spectra of Pt/rutile and Pt/anatase, TEM-images of rutile and anatase, STEM-images of 0.25Pt/anatase, CO light-off curves of Pt/rutile and Pt/anatase during CO oxidation TPRx, TOF and steady-state reaction order for CO during CO oxidation at 80 °C, STEM-images of 0.5Pt/rutile, 1Pt/rutile and 1Pt/anatase, XPS spectra of 1Pt/rutile, 1Pt/anatase, bare rutile and anatase, TOF for CO oxidation with varying CO concentration and fixed O2 concentration in 0.1Pt, 1Pt/rutile and anatase, 2D-rafted structure and 3D structure in 0.1Pt/rutile and 0.1Pt/anatase from STEM images (PDF)

■ AUTHOR INFORMATION

Corresponding Author

Ja Hun Kwak − *School of Energy and Chemical Engineering, Ulsan National Institute of Science and Technology (UNIST), Ulsan 44919, Republic of Korea; Center for Multidimensional Carbon Materials (CMCM), Institute for Basic Science (IBS), Ulsan 44919, Republic of Korea;* orcid.org/0000-0001-5245-0765; Email: jhkwak@unist.ac.kr

Authors

Haneul Kim − *School of Energy and Chemical Engineering, Ulsan National Institute of Science and Technology (UNIST), Ulsan 44919, Republic of Korea; Center for Multidimensional Carbon Materials (CMCM), Institute for Basic Science (IBS), Ulsan 44919, Republic of Korea;* orcid.org/0000-0003-1530-4579

Kwang Hyun Kim − *School of Energy and Chemical Engineering, Ulsan National Institute of Science and Technology (UNIST), Ulsan 44919, Republic of Korea; Center for Multidimensional Carbon Materials (CMCM), Institute for Basic Science (IBS), Ulsan 44919, Republic of Korea*

Konstantin Khivantsev − *Institute for Integrated Catalysis, Pacific Northwest National Laboratory, Richland, Washington 99352, United States;* orcid.org/0000-0002-4810-586X

Joonwoo Kim − *Industrial Gas Research Team, Research Institute of Industrial Science & Technology (RIST), Gwangyang-si, Jeollanam-do 57801, Republic of Korea*

Jaekyoung Lee − *Department of Chemical Engineering, Pukyong National University, Busan 48513, Republic of Korea*

Author Contributions

H.K.: synthesis and characterization of catalysts; data analysis; visualization; writing—original draft. K.H.K.: catalyst characterization (supporting). K.K.: review and editing (equal). J.K.: resources (equal). J.L.: visualization (supporting); review and editing (supporting). J.H.K.: supervision; conceptualization; resources (equal); data analysis; review and editing (equal); project administration. All authors contributed to this work and have approved the final version of the manuscript.

Notes

The authors declare no competing financial interest.

■ ACKNOWLEDGMENTS

This work was supported by the National Research Foundation of Korea (NRF- 2022R1F1A1076522, RS-2024-00343146), funded by the Korea government (MSIT). Experiments of the HAADF-STEM were supported in part by UNIST-UCRF. This work was also supported by the Institute for Basic Science (IBS-R019-D1). Experiments of the XPS were supported in part by KBSI. K.K. was supported by the U.S. Department of Energy, Office of Science, Basic Energy Sciences, Chemical Sciences, Geosciences, and Biosciences Division. Impact of catalytically active centers and their environment on rates and thermodynamic states along reaction paths. FWP 47319. PNNL is a multiprogram national laboratory operated for Department of Energy (DOE) by Battelle.

■ REFERENCES

(1) Suranovic, S. Fossil fuel addiction and the implications for climate change policy. *Glob. Environ. Change.* **2013**, *23* (3), 598−608.

(2) Abas, N.; Kalair, A.; Khan, N. Review of fossil fuels and future energy technologies. *Futures* **2015**, *69*, 31−49.

(3) Oh, D. G.; Aleksandrov, H. A.; Kim, H.; Koleva, I. Z.; Khivantsev, K.; Vayssilov, G. N.; Kwak, J. H. Key Role of a-Top CO on Terrace Sites of Metallic Pd Clusters for CO Oxidation. *Chem.—Eur. J.* **2022**, *28* (49), No. e202200684.

(4) Owusu, P. A.; Asumadu-Sarkodie, S.; Dubey, S. A review of renewable energy sources, sustainability issues and climate change mitigation. *Cogent Eng.* **2016**, *3* (1), 1167990.

(5) Ngorot Kembo, J. P.; Wang, J.; Luo, N.; Gao, F.; Yi, H.; Zhao, S.; Zhou, Y.; Tang, X. A review of catalytic oxidation of carbon monoxide over different catalysts with an emphasis on hopcalite catalysts. *New J. Chem.* **2023**, *47* (44), 20222−20247.

(6) Wilbur, S.; Williams, M.; Williams, R.; Scinicariello, F.; Klotzbach, J. M.; Diamond, G. L.; Citra, M. *Toxicological Profile for Carbon Monoxide*; Atlanta (GA), 2012.

(7) Lee, J.; Jang, E. J.; Oh, D. G.; Szanyi, J.; Kwak, J. H. Morphology and size of Pt on Al2O3: The role of specific metal-support interactions between Pt and Al_2O_3. *J. Catal.* **2020**, *385*, 204−212.

(8) Jang, E. J.; Kim, E.; Oh, D. G.; Kim, Y.; Jeon, J. H.; Han, H. S.; Kim, J. M.; Lee, J.; Kwak, J. H. Promotional effect of Mn on Pt/Al_2O_3 catalysts in HC, CO, and NOx oxidation for controlling diesel emission. *Catal. Today* **2024**, *425*, 114300.

(9) Ivanova, A. S.; Slavinskaya, E. M.; Gulyaev, R. V.; Zaikovskii, V. I.; Stonkus, O. A.; Danilova, I. G.; Plyasova, L. M.; Polukhina, I. A.; Boronin, A. I. Metal−support interactions in Pt/Al_2O_3 and Pd/Al_2O_3 catalysts for CO oxidation. *Appl. Catal., B* **2010**, *97* (1−2), 57−71.

(10) Oh, D. G.; Aleksandrov, H. A.; Kim, H.; Koleva, I. Z.; Khivantsev, K.; Vayssilov, G. N.; Kwak, J. H. Understanding of Active Sites and Interconversion of Pd and PdO during CH_4 Oxidation. *Molecules* **2023**, *28* (4), 1957.

(11) Haneda, M.; Watanabe, T.; Kamiuchi, N.; Ozawa, M. Effect of platinum dispersion on the catalytic activity of Pt/Al_2O_3 for the oxidation of carbon monoxide and propene. *Appl. Catal., B* **2013**, *142−143*, 8−14.

(12) An, N.; Yuan, X.; Pan, B.; Li, Q.; Li, S.; Zhang, W. Design of a highly active Pt/Al_2O_3 catalyst for low-temperature CO oxidation. *RSC Adv.* **2014**, *4* (72), 38250−38257.

(13) Lin, J.; Wang, X.; Zhang, T. Recent progress in CO oxidation over Pt-group-metal catalysts at low temperatures. *Chin. J. Catal.* **2016**, *37* (11), 1805−1813.

(14) Taira, K.; Nakao, K.; Suzuki, K.; Einaga, H. SOx Tolerant Pt/TiO_2 Catalysts for CO Oxidation and the Effect of TiO2 Supports on Catalytic Activity. *Environ. Sci. Technol.* **2016**, *50* (17), 9773−9780.

(15) Lane, G.; Wolf, E. Characterization and Fourier transform infrared studies of the effects of TiO_2 crystal phases during CO oxidation on Pt/TiO_2 catalysts. *J. Catal.* **1987**, *105* (2), 386−404.

(16) Nagai, Y.; Dohmae, K.; Ikeda, Y.; Takagi, N.; Tanabe, T.; Hara, N.; Guilera, G.; Pascarelli, S.; Newton, M. A.; Kuno, O.; et al. In situ redispersion of platinum autoexhaust catalysts: An on-line approach to increasing catalyst lifetimes? *Angew. Chem., Int. Ed.* **2008**, *47* (48), 9303−9306.

(17) Nagai, Y.; Hirabayashi, T.; Dohmae, K.; Takagi, N.; Minami, T.; Shinjoh, H.; Matsumoto, S. Sintering inhibition mechanism of platinum supported on ceria-based oxide and Pt-oxide−support interaction. *J. Catal.* **2006**, *242* (1), 103−109.

(18) Yang, Z.; Zhang, N.; Cao, Y.; Li, Y.; Liao, Y.; Li, Y.; Gong, M.; Chen, Y. Promotional effect of lanthana on the high-temperature thermal stability of Pt/TiO_2 sulfur-resistant diesel oxidation catalysts. *RSC Adv.* **2017**, *7* (31), 19318−19329.

(19) Liu, J.; Ding, T.; Zhang, H.; Li, G.; Cai, J.; Zhao, D.; Tian, Y.; Xian, H.; Bai, X.; Li, X. Engineering surface defects and metal−support interactions on Pt/TiO_2(B) nanobelts to boost the catalytic oxidation of CO. *Catal. Sci. Technol.* **2018**, *8* (19), 4934−4944.

(20) Ivanova, E.; Mihaylov, M.; Thibault-Starzyk, F.; Daturi, M.; Hadjiivanov, K. FTIR spectroscopy study of CO and NO adsorption and co-adsorption on Pt/TiO_2. *J. Mol. Catal. A: Chem.* **2007**, *274* (1−2), 179−184.

(21) Zafiris, G. S.; Gorte, R. J. CO Oxidation on Pt/α-Al_2O_3(0001): Evidence for Structure Sensitivity. *J. Catal.* **1993**, *140* (2), 418−423.

(22) Li, N.; Chen, Q.-Y.; Luo, L.-F.; Huang, W.-X.; Luo, M.-F.; Hu, G.-S.; Lu, J.-Q. Kinetic study and the effect of particle size on low temperature CO oxidation over Pt/TiO_2 catalysts. *Appl. Catal., B* **2013**, *142−143*, 523−532.

(23) DeRita, L.; Dai, S.; Lopez-Zepeda, K.; Pham, N.; Graham, G. W.; Pan, X.; Christopher, P. Catalyst Architecture for Stable Single Atom Dispersion Enables Site-Specific Spectroscopic and Reactivity Measurements of CO Adsorbed to Pt Atoms, Oxidized Pt Clusters, and Metallic Pt Clusters on TiO_2. *J. Am. Chem. Soc.* **2017**, *139* (40), 14150−14165.

(24) Thang, H. V.; Pacchioni, G.; DeRita, L.; Christopher, P. Nature of stable single atom Pt catalysts dispersed on anatase TiO_2. *J. Catal.* **2018**, *367*, 104−114.

(25) Dessal, C.; Len, T.; Morfin, F.; Rousset, J.-L.; Aouine, M.; Afanasiev, P.; Piccolo, L. Dynamics of Single Pt Atoms on Alumina during CO Oxidation Monitored by Operando X-ray and Infrared Spectroscopies. *ACS Catal.* **2019**, *9* (6), 5752−5759.

(26) Altman, E. I.; Gorte, R. J. A study of small Pt particles on amorphous Al_2O_3 and α-Al_2O_3{0001} substrates using TPD of CO and H_2[1]. *J. Catal.* **1988**, *110* (1), 191−196.

(27) Gracia, F. J.; Bollmann, L.; Wolf, E. E.; Miller, J. T.; Kropf, A. J. In situ FTIR, EXAFS, and activity studies of the effect of crystallite size on silica-supported Pt oxidation catalysts. *J. Catal.* **2003**, *220* (2), 382−391.

(28) Gracia, F. J.; Miller, J. T.; Kropf, A. J.; Wolf, E. E. Kinetics, FTIR, and Controlled Atmosphere EXAFS Study of the Effect of

Chlorine on Pt-Supported Catalysts during Oxidation Reactions. *J. Catal.* **2002**, *209* (2), 341−354.
(29) Kim, Y.; Oh, D. G.; Cho, S. J.; Khivantsev, K.; Kwak, J. H. Catalytic behavior of Pt single-atoms supported on CeO_2. *Catal. Today* **2024**, *425*, 114298.
(30) Kim, Y.; Collinge, G.; Lee, M. S.; Khivantsev, K.; Cho, S. J.; Glezakou, V. A.; Rousseau, R.; Szanyi, J.; Kwak, J. H. Surface Density Dependent Catalytic Activity of Single Palladium Atoms Supported on Ceria*. *Angew. Chem., Int. Ed.* **2021**, *60* (42), 22769−22775.
(31) Watanabe, Y.; Wu, X.; Hiratac, H.; Isomura, N. Size-dependent catalytic activity and geometries of size-selected Pt clusters on TiO2(110) surfaces. *Catal. Sci. Technol.* **2011**, *1* (8), 1490−1495.
(32) Casapu, M.; Fischer, A.; Gänzler, A. M.; Popescu, R.; Crone, M.; Gerthsen, D.; Türk, M.; Grunwaldt, J.-D. Origin of the Normal and Inverse Hysteresis Behavior during CO Oxidation over Pt/Al_2O_3. *ACS Catal.* **2017**, *7* (1), 343−355.
(33) Chen, Y.; Feng, Y.; Li, L.; Liu, J.; Pan, X.; Liu, W.; Wei, F.; Cui, Y.; Qiao, B.; Sun, X.; et al. Identification of Active Sites on High-Performance Pt/Al_2O_3 Catalyst for Cryogenic CO Oxidation. *ACS Catal.* **2020**, *10* (15), 8815−8824.
(34) Neumann, S.; Gutmann, T.; Buntkowsky, G.; Paul, S.; Thiele, G.; Sievers, H.; Bäumer, M.; Kunz, S. Insights into the reaction mechanism and particle size effects of CO oxidation over supported Pt nanoparticle catalysts. *J. Catal.* **2019**, *377*, 662−672.
(35) Beniya, A.; Higashi, S.; Ohba, N.; Jinnouchi, R.; Hirata, H.; Watanabe, Y. CO oxidation activity of non-reducible oxide-supported mass-selected few-atom Pt single-clusters. *Nat. Commun.* **2020**, *11* (1), 1888.
(36) Kim, H.; Kim, J.; Kwak, J. H. Origin of Higher CO Oxidation Activity of Pt/Rutile than That of Pt/Anatase. *J. Phys. Chem. C* **2023**, *127* (15), 7142−7150.
(37) Oh, S.; Ha, H.; Choi, H.; Jo, C.; Cho, J.; Choi, H.; Ryoo, R.; Kim, H. Y.; Park, J. Y. Oxygen activation on the interface between Pt nanoparticles and mesoporous defective TiO_2 during CO oxidation. *J. Chem. Phys.* **2019**, *151* (23), 234716.
(38) Ding, K.; Gulec, A.; Johnson, A. M.; Schweitzer, N. M.; Stucky, G. D.; Marks, L. D.; Stair, P. C. Identification of active sites in CO oxidation and water-gas shift over supported Pt catalysts. *Science* **2015**, *350* (6257), 189−192.
(39) Ruiz Puigdollers, A.; Schlexer, P.; Tosoni, S.; Pacchioni, G. Increasing Oxide Reducibility: The Role of Metal/Oxide Interfaces in the Formation of Oxygen Vacancies. *ACS Catal.* **2017**, *7* (10), 6493−6513.
(40) Anderson, J. R.; Boudart, M.; Schwab, G. M.; Emmett, P. H.; Fromment, G. F. *Catalysis*; Springer: Berlin Heidelberg, 1984.
(41) Benson, J.; Boudart, M. Hydrogen-oxygen titration method for the measurement of supported platinum surface areas. *J. Catal.* **1965**, *4* (6), 704−710.
(42) Boudart, M.; Rumpf, F. The catalytic oxidation of CO and structure insensitivity. *React. Kinet. Catal. Lett.* **1987**, *35* (1−2), 95−105.
(43) Cant, N. Metal crystallite size effects and low-temperature deactivation in carbon monoxide oxidation over platinum. *J. Catal.* **1980**, *62* (1), 173−175.
(44) Allian, A. D.; Takanabe, K.; Fujdala, K. L.; Hao, X.; Truex, T. J.; Cai, J.; Buda, C.; Neurock, M.; Iglesia, E. Chemisorption of CO and mechanism of CO oxidation on supported platinum nanoclusters. *J. Am. Chem. Soc.* **2011**, *133* (12), 4498−4517.
(45) Cargnello, M.; Doan-Nguyen, V. V.; Gordon, T. R.; Diaz, R. E.; Stach, E. A.; Gorte, R. J.; Fornasiero, P.; Murray, C. B. Control of metal nanocrystal size reveals metal-support interface role for ceria catalysts. *Science* **2013**, *341* (6147), 771−773.
(46) Anderson, J. A. CO Oxidation over Alumina Supported Platinum Catalyst. *Catal. Lett.* **1992**, *13* (4), 363−369.
(47) Tesvara, C.; Yousuf, M. R.; Albrahim, M.; Troya, D.; Shrotri, A.; Stavitski, E.; Karim, A. M.; Sautet, P. Unraveling the CO Oxidation Mechanism over Highly Dispersed Pt Single Atom on Anatase TiO_2 (101). *ACS Catal.* **2024**, *14*, 7562−7575.